Supplementary Information for

# *Lubricity, Wear Prevention, and Anti-Biofouling Properties of Macromolecular Coatings for Endotracheal Tubes*

*Bernardo Miller Naranjo, Michael Zollo, Stephan A. Sieber and Oliver Lieleg**

B. Miller Naranjo, Oliver Lieleg

TUM School of Engineering and Design Department of Materials Engineering

Technical University of Munich (TUM)

Boltzmannstraße 15, 85748 Garching, Germany

E-mail: oliver.lieleg@tum.de

B. Miller Naranjo, Oliver Lieleg

Center for Protein Assemblies (CPA) and Munich Institute of Biomedical Engineering (MIBE)

Technical University of Munich (TUM)

Ernst-Otto-Fischer Straße 8, 85748 Garching, Germany

M. Zollo, S. A. Sieber

TUM School of Natural Sciences, Department of Bioscience, Chair of Organic Chemistry II

Center for Functional Protein Assemblies (CPA)

Technical University of Munich (TUM)

Ernst-Otto-Fischer-Str. 8, Garching 85748, Germany

**Section S1: Selecting alternative macromolecules**

In this study, we explore the possibility to substitute porcine gastric mucins as macromolecular components to generate lubricating, anti-biofouling coatings on ETTs. Whereas mucins show a broad range of functionalities, their use is restricted for certain parts of society. For instance, some people who will avoid such porcine mucins due to religious reasons (*e.g.*, the Jewish and Muslim community), whereas others will avoid such mucins since they follow a vegan lifestyle. To identify a set of macromolecules to generate alternative coatings from, we conducted pre-tests with 5 different macromolecular coatings created from HA, PEG60, PEG100, L-Dex, and Chitosan. Based on the performance of those coatings in terms of providing lubricity (**Figure S1a**) and improving the wetting properties of ETTs (**Figure S1b**) and with the considerations above, using another animal product such as chitosan did not seem to be the best option. Thus, we selected the subset of 3 macromolecules studied in detail in the main text.

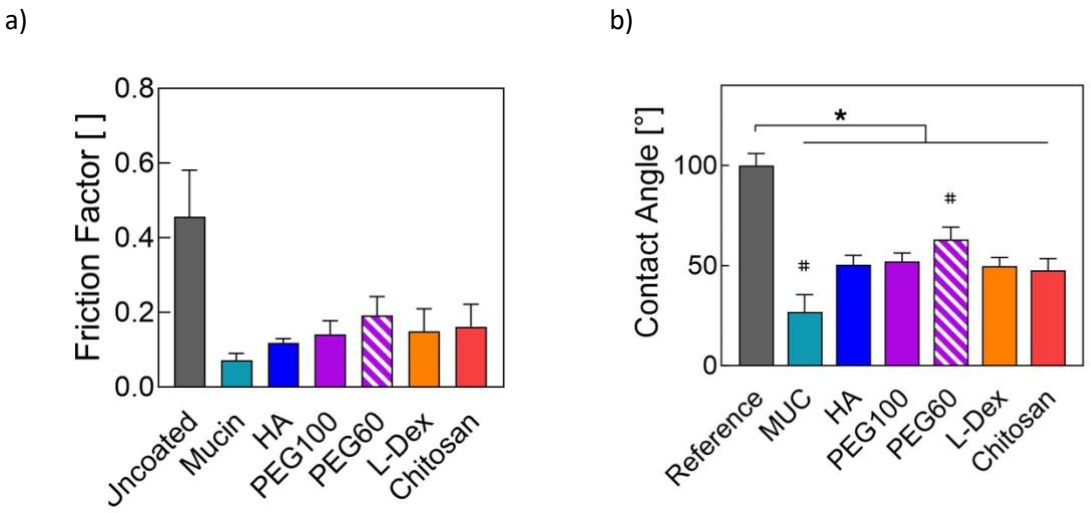


**Figure S1**. Friction reduction and wettability enhancement as achieved by different macromolecular coatings. a) Friction factor measured in a steel-on-PDMS at a sliding speed of 15 mm/s. The measurements were conducted using a commercial rheometer equipped with a tribology unit using a ball-on-3-pins geometry. Measurements were conducted for $n = 3$ independent samples. Owing to the small sample size, significance tests were not applied to those tribological measurements. b) Contact angles determined for ETTs coated with the same set of macromolecules as in a). The contact angle was measured at least $n = 15$ times on 9 independent samples per condition. Asterisks (*) and rhombi (#) denote significant differences (based on a p-value of $p = 0.05$) when comparing a coating to uncoated ETTs (analyzed *via* a 2-sample t-test) or when comparing the different coatings among each other (tested *via* an ANOVA and Tukey post-hoc test), respectively.

**Section S2: Estimation of the water binding abilities of the different macromolecules**

To approximate the amount of water molecules each of the macromolecules studied here can bind, we conducted measurements using cell culture inserts (CellQart, SABEU GmbH & Co. KG, Northeim, Germany) as follows (see **Figure S2**): 1 mg of each macromolecule type was weighed into a clean and fresh cell culture insert, which was subsequently positioned in one of the wells of a 48-well plate. Then, 1 mL of dd$H_2O$ was carefully pipetted into the well and the well plate was hermetically closed. The spaces between the wells were filled with an ethanol solution to reduce evaporation effects. Then, the wells were incubated over night to allow for water to be sucked past the membrane of the cell culture insert into the compartment carrying the macromolecules. To ensure that saturating conditions were reached, another dose of 1 mL of water was added and the wells were stored for another day. Then, each cell culture insert was transferred into an empty well to allow for unbound water to drip off. After 15 minutes, the cell culture inserts were weighed once more to determine the change in mass caused by the uptake of water. An approximate molecular weight of the macromolecules (as reported in **Figure 1b** of the main paper) was then used to calculate the amount of water molecules bound by each macromolecule.

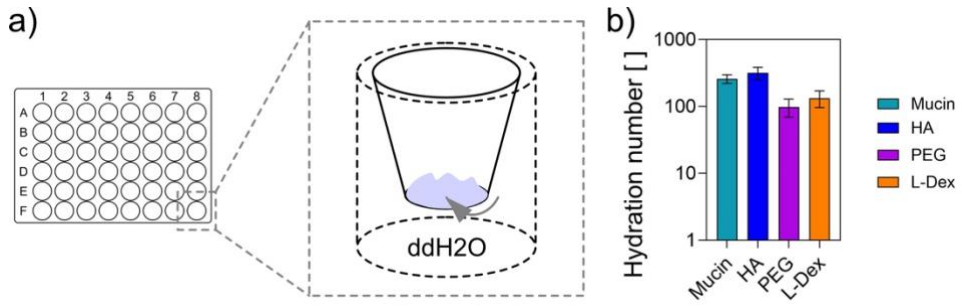


***Figure S2.*** Approximation of the hydration number, *i.e.*, the number of water molecules bound per macromolecule. a) Schematic representation of the measuring approach. b) Calculated results for the hydration number of the different macromolecules. Bars denote the mean error bars the standard deviation as calculated from $n = 3$ independent measurements.

**Section S3: Homogeneity and thickness of different macromolecular coatings**

To visualize the generated coatings and to estimate their thickness, the macromolecules were labelled with a fluorophore using carbodiimide chemistry as described previously by Rickert et. al.[1]. Then, images of the coatings were acquired using confocal microscopy. [2]

In brief, starting from a stock solution, a 10 mg/mL dye (ATTO495 carboxy modified, ATTO-TEC GmbH, Siegen, Germany) solution was diluted in 10 mM MES buffer (pH 5.0) to a final concentration of 1 mg/mL. Then, EDC and sulfo-NHS were added until a concentration of 5 mM each was reached. The mixture was incubated at room temperature for 3 h while avoiding exposure to light. During this incubation step, 40 mg of macromolecule were dissolved in 19 mL of phosphate saline buffer (PBS, pH 7.0). Then, 1 mL of the dye containing solution was mixed into each macromolecule solution. After an incubation time of 3 h, the solution was dialyzed (MWCO = 80 kDa) against dd$H_2O$ before being lyophilized and stored at -80 °C until further use.

Owing to differences in the molecular structure of HA, however, this labelling procedure requires minor modifications. First, the ATTO dye used here is an amino modified variant (ATTO495 amino modified). Second, the EDC-NHS modification needs to start at the carboxyl groups present in the HA macromolecule. Accordingly, 40 mg of HA were dissolved in 19 mL MES buffer (pH 5.0) and EDC and NHS were added to this solution until a concentration of 200 mM EDC and 50 mM NHS was reached. This solution was incubated on a rolling shaker for 3 h at room temperature. Finally, the solution containing the (amine-modified) ATTO dye was added and, after 3 h of incubation at room temperature, the solution was dialyzed (MWCO = 80 kDa) against ultrapure water before being lyophilized and stored at –80 °C.

Coatings were generated from the fluorescently labelled macromolecules as described in the main paper; now, special care was taken to avoid light exposure during all coating steps.

A visualization of the generated coatings was achieved *via* confocal microscopy on a Leica TCS SP8 setup (Leica, Wetzlar, Germany) equipped with a DMI-8 corpus (Leica) and a 40x objective (HCX PL APO; NA = 1.25, Leica). The fluorophores were excited at 495 nm and emission was detected in a wavelength range from 510 to 540 nm. The z-dimension was then scanned with a step-size of 0.1 µm and an image was recorded after each step in z-direction (**Figure S3a**). This discrete scan of a curved surface in z-direction is, in part, responsible for the pattern shown in **Figure S3a**. In addition, the surface of the commercial ETTs is not perfectly smooth. Those imperfections can even be identified by the naked eye when holding a sample against artificial light (**Figure S3b**). In addition, a profilometric image (**Figure S3c**) of

the outer surface of an ETT sample clearly shows a linear pattern present on the surface. This pattern is probably a result of the ETT production process and is maintained when a macromolecular coating is applied.

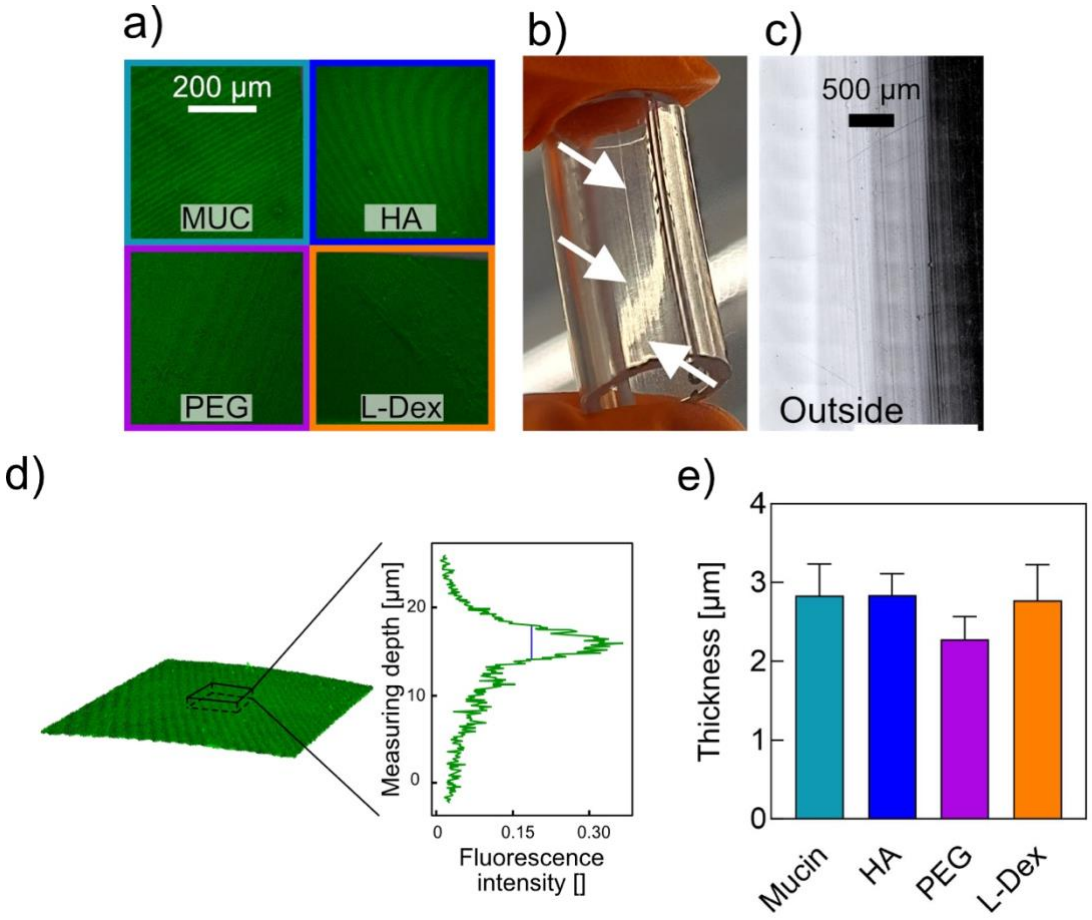


***Figure S3.*** Homogeneity and estimated thickness of the coatings. a) Overview of the coated ETT samples. The stripey pattern in the obtained images results from a structural feature present on the surface of the ETTs. The scale bar denotes 200 µm and applies to all four images. b) shows a picture taken with a digital camera. A section of an ETT is held against artificial light so that the surface structure caused by the production process becomes visible. c) Profilometric image of the outer surfaces of an ETTs imaged with 20x magnification. The scale bar represents 500 µm. d) Approximation of the coating thickness. The fluorescence intensity is recorded for the measurement depth. From that signal, the full width at half maximum (FWHM) is used as an approximation of the coating thickness. e) Results of the calculated thicknesses are depicted as the mean with the standard deviation, which was calculated from $n = 3$ independent samples for each of the conditions we studied.

The obtained rgb image stack was converted to grayscale and the mean intensity was calculated for each of the images. With this approach, a curve denoting the fluorescence intensity over the

measuring depth is obtained as shown in **Figure S3d**. Then, the full width at half maximum (FWHM) was used as an approximation of the thickness of the coating.

To avoid a distortion of the intensity curves caused by the curvature of the ETTs, the FWHM was calculated on 25 random 3x3 pixel squares of each of the images and the obtained average was reported as an estimate of the coating thickness for each of the samples. **Figure S3e** shows that, for all coatings, a thickness in the range of a few µm was achieved. All calculations were conducted using python (Python Software Foundation; Python Language Reference, version 3.9.12; http://www.python.org) [3] with the NumPy (v1.20.3) [4] extension for data handling and the SciPy (v1.7.3) [5] plugin for data analysis.

It should be mentioned that the fluorescence-based method we use here is susceptible to cross-illumination and other effects. Therefore, the thickness values we report here are only an approximation. Still, our results do show that the coatings are thin, homogenous, and reproducible.

**Section S4: Friction measurements on ETT coatings**

Friction tests on ETT coatings were conducted using a steel-on-ETT setup in a commercial rheometer equipped with a tribology unit as described in the main paper. In **Figure S4,** the full obtained friction curves are shown. From those curves, the bar plots shown in Figure 3 of the main paper were generated.

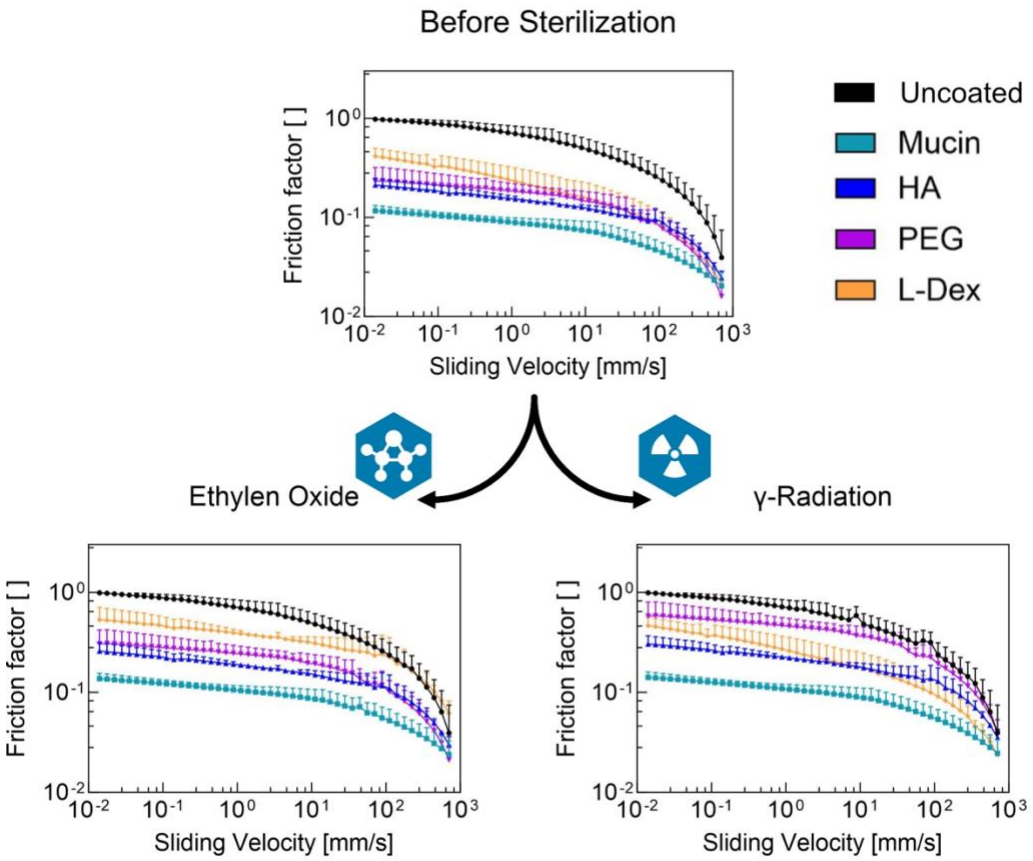


***Figure S4.*** Rotational tribology measurements. Differently coated ETT samples were tested on a tribology setup to determine the friction factor in a steel-on-ETT pairing before and after sample sterilization *via* ethylene oxide fumigation and γ-irradiation, respectively. Data shown represents averages from $n$ = 3 independent samples; error bars denote the standard deviation.

**Section S5: Tissue damage determination**

As described previously[2], trachea samples were purchased from a local butcher, freed from adjacent tissue, cut into pieces of 5 cm in length, and then slit open to allow for a tissue damage analysis *via* a two-step trypan blue (TB) staining and subsequent image analysis.

In brief, after tissue preparation (as described in the main text), the tracheal samples were stained for 40 minutes in a trypan blue solution (which was prepared at a concentration of 0.01 % in PBS). We then acquired an image of the tracheal samples inside of a photo cube (Caruba, Bathoorn, Sweden) at a defined distance of about 40 cm using a digital camera (Canon EOS M50 Mark II, Tokyo, Japan). The photo box has its own light source, which we adjusted to maximum intensity. After conducting the extubation test, we repeated the staining and image acquisition steps. Thus, we now had a pair of pictures: one describing the state of a tissue sample before and one describing the state of the tissue sample after exposure to tribological stress. Exemplary image pairs obtained with this procedure before and after the extubation test are shown in **Figure S5**.

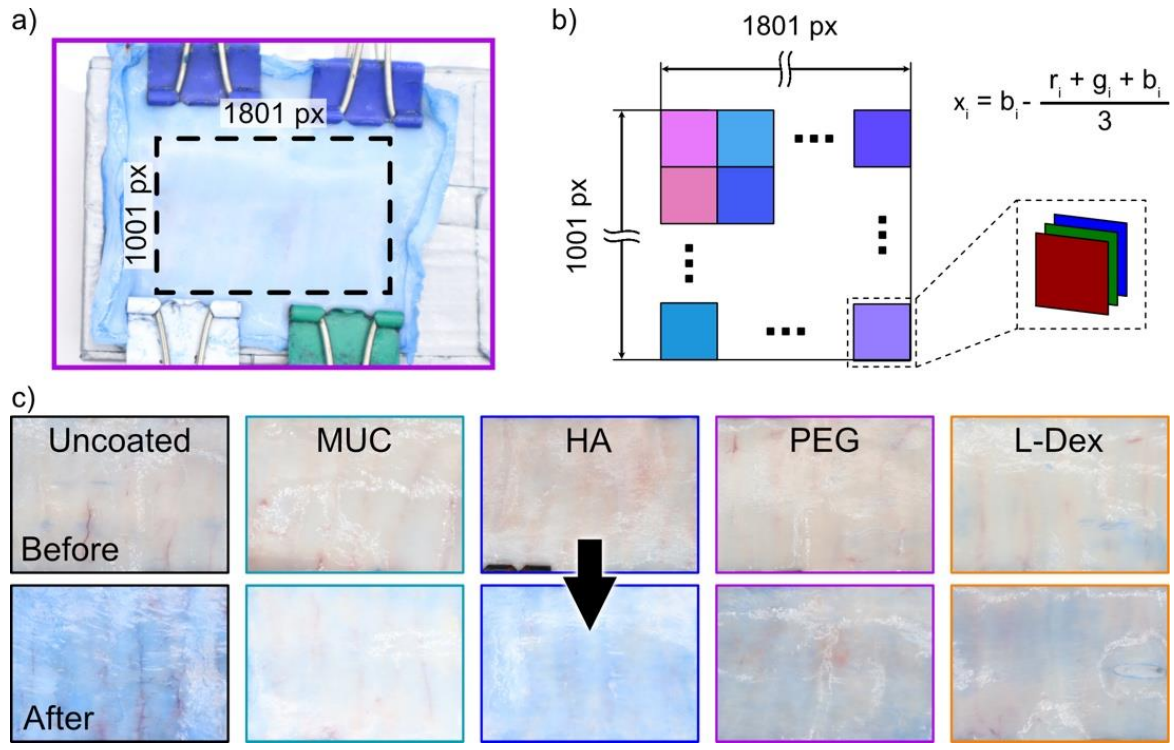


***Figure S5***. Tissue damage assessment via Trypan Blue (TB) staining and subsequent image quantification. a) Images from TB-stained tracheal samples were acquired before and after tribological treatment, and a 1801-by-1001 pixel portion of each image was analyzed. $n$ = 9 independent tissue samples were studied per condition. b) A pixel-by-pixel analysis was conducted to quantify the level of blue dominance of each image. In subfigure c), exemplary images are shown for the different experimental groups; images in the upper row were obtained before, and images in the lower row were obtained after the extubation procedure.

We then conducted a pixel-by-pixel analysis, for which we defined a running variable $x_i$ that gives a measure for the blue dominance in a pixel. To obtain this parameter, we extracted the rgb values for each pixel and subtracted their average from the blue value of that pixel. With this approach, we obtained positive $x_i$ values for pixels that are blue dominated and negative values for pixels that are not. Reflections produced by the light source on the smooth trachea surface were automatically filtered out, since the $x_i$ value for such pixels is 0 (r, g, b are all 255 for white pixels). By averaging over all $x_i$ values determined from each of the two images and calculating the difference of those two averages, we obtained a parameter that reflects the level of tissue damage inflicted to this particular tissue sample by the tribological extubation treatment.

**Section S6: Cell colonization tests**

First, a cytotoxicity test was conducted by growing HeLa cells in accordance with the norm ISO 10993. For this purpose, ETT samples of ~1 cm in length were coated with the different macromolecules; as a control, uncoated samples were prepared. These samples were then thoroughly rinsed in sterile PBS and exposed to UV light for 30 min (BLX-254, Vilber Lourmat GmbH, Eberhardzell, Germany). The samples were then placed into 3 mL of sterile cell medium and incubated for 24 h at 37 °C and 5 % (v/v) $CO_2$. With this procedure, we produced a "leaching" medium for each coating type, to which we exposed HeLa cells in a second step. Here, HeLa cells were seeded into a 96 well-plate. 8 wells containing 5000 cells and 100 µL of standard medium were prepared for each condition tested. After 24 h of incubation, 50 µL of the cell medium were substituted with 50 µL of the "leaching" medium, and the cell viability was assessed *via* a WST-1 assay, as described in the main paper.

The obtained results are shown in **Figure S6a** and demonstrate that none of the coatings had released cytotoxic components.

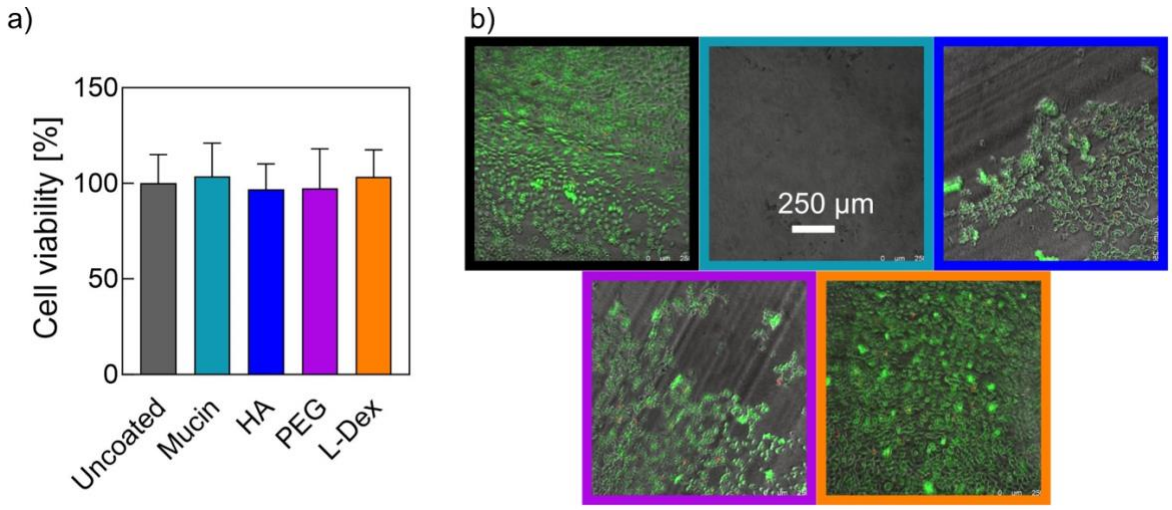


***Figure S6.*** Cytotoxicity and anti-biofouling tests conducted with HeLa cells. a) Cytotoxicity tests were conducted *via* leaching assay. Bars denote the mean and the error bars the standard deviation as calculated from $n$ = 8 independent samples. b) Exemplary images of cell colonization tests. HeLa cells were seeded onto coated and uncoated ETT samples, respectively. Exemplary images show how the different coatings differ in their ability to mitigate cell adhesion. The scale bar shown in the second image applies to all images in this figure.

To support the findings obtained from a WST (Figure 2c of the main text), HeLa cells were seeded onto ETT samples carrying different coatings and subjected to a live/dead staining as described in the main text. Images of the stained cells were obtained using fluorescence microscopy, and exemplary images are shown below in **Figure S6b**.

**Section S7: Bacterial colonization tests**

In addition to the tests described in the main text, we also conducted bacterial colonization tests with the strain *P. aeruginosa*. The corresponding results are shown in **Figure S7** and demonstrate that, for this particular strain, none of the coatings was able to significantly reduce the number of bacteria adhering to the ETT surface – not even mucin.

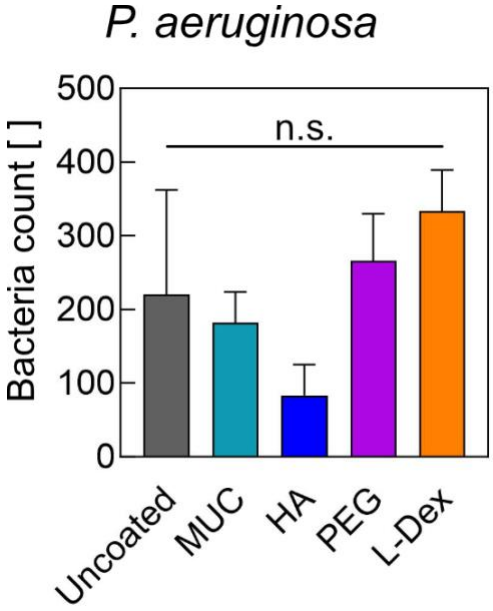


***Figure S7***. Bacterial colonization of different ETT surface after incubated with a solution containing planktonic bacteria of the strain *P. aeruginosa*. Error bars denote the standard deviation as determined from $n = 9$ independent samples.

## Section S8: Lipid deposition tests

To study the anti-biofouling properties of the coatings, ETT samples carrying the different macromolecular coatings were exposed to a lipid solution. **Figure S8** shows exemplary images of the samples after being incubated in the lipid solution.

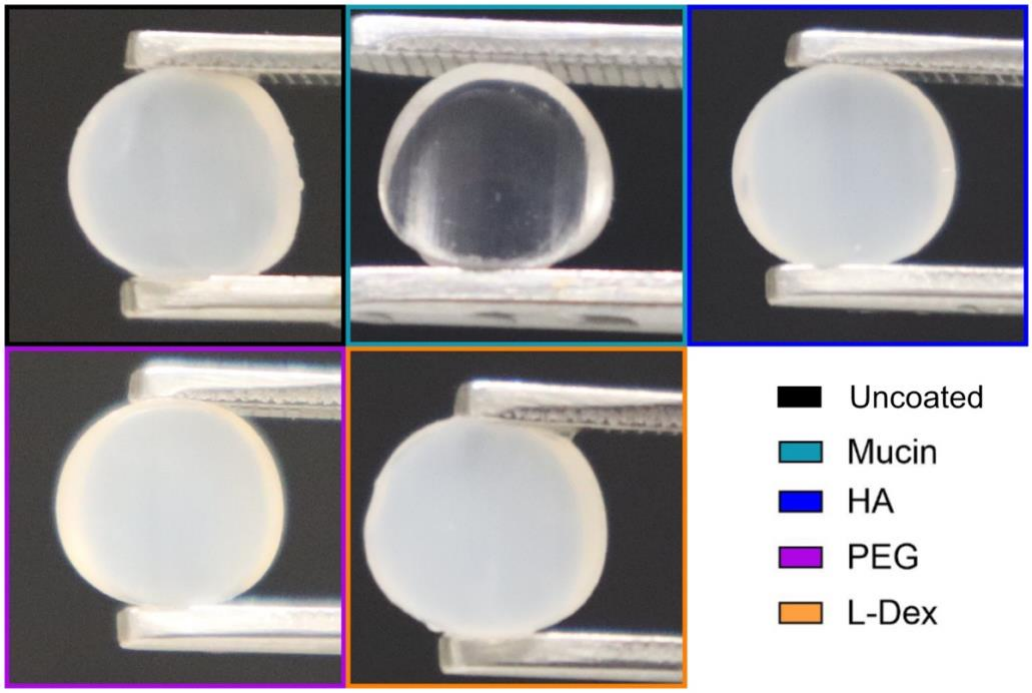


***Figure S8.*** Exemplary images of the lipid deposition tests. Cylindrical ETT samples (diameter 7 mm) carrying different coatings were exposed to a lipid solution. Exemplary images show how the coatings differ in their ability to mitigate lipid deposition.

## Section S9: Protein deposition tests

To study the anti-biofouling properties of the coatings, ETT samples carrying the different macromolecular coatings were exposed to a BSA solution. **Figure S9** shows exemplary images of the samples after being incubated in the BSA solution.

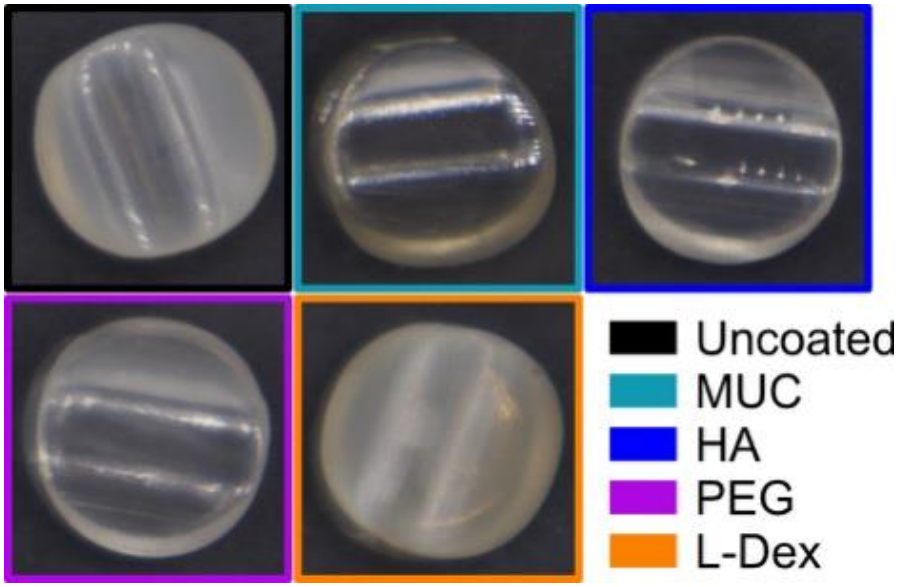


**Figure S9.** Exemplary images of the protein (BSA) adsorption tests. Cylindrical ETT samples (diameter 7 mm) carrying different coatings were exposed to a BSA solution. Exemplary images show how the coatings differ in their ability to mitigate BSA adsorption.

**Section S10: Long-term storage**

Between the process of coating and terminal sterilization and final usage of the ETTs, storage times need to be taken into account. We therefore conducted measurements (CA and friction factor) after 1, 4, and 8 weeks to assess the long-term stability of the coatings in both, dry and wet storing conditions. The results presented in **Figure S10** show that the coatings remain stable and functional after 8 weeks.

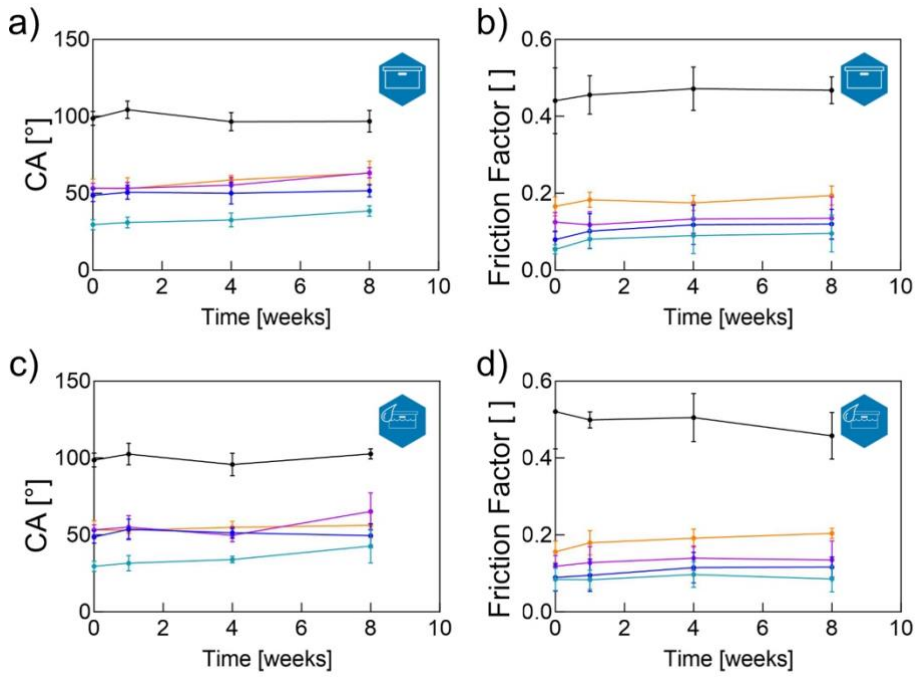


***Figure S10***. Long term stability. Contact angle (CA) and friction factor measurements were conducted as proof of the presence and functionality of the coatings in dry storage conditions at room temperature (a, b), and in phosphate buffered saline (PBS) solution (c, d) after 1, 4, and 8 weeks. Measurement points show the mean, and the error bars denote the standard deviation as calculated from $n = 3$ independent samples.

**Cited Literature:**

(1) Rickert, C. A.; Wittmann, B.; Fromme, R.; Lieleg, O. Highly transparent covalent mucin coatings improve the wettability and tribology of hydrophobic contact lenses. *ACS applied materials & interfaces* **2020**, *12* (25), 28024-28033.
(2) Miller Naranjo, B.; Naicker, S.; Lieleg, O. Macromolecular Coatings for Endotracheal Tubes Probed on An Ex Vivo Extubation Setup. *Advanced Materials Interfaces n/a* (n/a), **2023**, 2201757. DOI: https://doi.org/10.1002/admi.202201757.
(3) Van Rossum, G.; Drake, F. Python 3 reference manual createspace. *Scotts Valley, CA* **2009**.
(4) Harris, C. R.; Millman, K. J.; Van Der Walt, S. J.; Gommers, R.; Virtanen, P.; Cournapeau, D.; Wieser, E.; Taylor, J.; Berg, S.; Smith, N. J. Array programming with NumPy. *Nature* **2020**, *585* (7825), 357-362.
(5) Virtanen, P.; Gommers, R.; Oliphant, T. E.; Haberland, M.; Reddy, T.; Cournapeau, D.; Burovski, E.; Peterson, P.; Weckesser, W.; Bright, J. SciPy 1.0: fundamental algorithms for scientific computing in Python. *Nature methods* **2020**, *17* (3), 261-272.